

One-Bit DoA Estimation for Deterministic Signals Based on $\ell_{2,1}$ -Norm Minimization

Correspondence

Abstract— One-bit direction of arrival (DoA) estimation has drawn considerable attention in recent years with the increasing demand for low power consumption and high sampling rate. In this work, the one-bit DoA estimation for deterministic signals is addressed from the viewpoint of sparse matrix recovery. First, using maximum likelihood (ML) and compressive sensing techniques, one-bit DoA estimation is formulated as an ML-based row sparse matrix optimization in terms of least-absolute-shrinkage-and-selection-operator form with a $\ell_{2,1}$ regularization. After that, by complex-valued conjugate gradient and steepest descent operations, an iterative closed-form solution in the form of row sparse matrix is expected to be obtained. At last, the estimates of source number and DoAs are simultaneously completed by making sense of the structure of the row sparse matrix. Numerical results showcase that the proposed algorithm outperforms the state-of-the-art approaches in terms of estimation accuracy.

Index Terms— One-bit quantization, sparse matrix recovery, direction of arrival (DoA) estimation, deterministic signals, $\ell_{2,1}$ -norm.

I. INTRODUCTION

DIRECTION of arrival (DoA) estimation using one-bit analog-to-digital converters (ADCs), namely, one-bit DoA estimation, has garnered substantial attention owing to its inherent advantages, such as remarkably low manufacturing costs, less energy consumption, efficient data transmission, and minimal data storage requirement in practical systems, which turns out to be a very promising technique for unmanned aerial vehicle (UAV) applications [1]–[3]. However, the highly nonlinear relationship between the source signal and the received signal caused by one-bit quantization brings new challenges to DoA estimation [4]. To tackle this issue, recent research has predominantly focused on two distinct categories of methods, i.e., subspace-based approaches and compressed

This work was supported in part by the National Science Fund for Distinguished Young Scholars under Grant 61925108, the Key Project of International Cooperation and Exchanges of the National Natural Science Foundation of China under Grant 62220106009, the project of Shenzhen Peacock Plan Teams under Grant KQTD20210811090051046, Shenzhen University 2035 Program for Excellent Research, the National Natural Science Foundation of China under Grant 62371306, and Guangdong Basic and Applied Basic Research Foundation under Grant 2021A1515011855. (*Corresponding author: Qiang Li; Lei Huang*).

M. Chen, Q. Li, X. P. Li are with the College of Electronics and Information Engineering, Shenzhen University, Shenzhen 518060, China (e-mail: mychen@139.com). L. Huang is with the State Key Laboratory of Radio Frequency Heterogeneous Integration (Shenzhen University), Shenzhen 518060, China (e-mail: lhuang@szu.edu.cn). M. Rihan is with the Department of Communications Engineering, University of Bremen, Bremen 28359, Germany. He is on leave from the Department of Communication Engineering, Faculty of Electronic Engineering, Menoufia University, Al-Menoufia, Egypt.

sensing (CS)-based techniques. Each holds its unique strengths and limitations.

Subspace-based methods rely on the Arcsine Law, discovered by Van-Vleck [5] and then extended to complex-valued signals by Jacovitti and Neri [6], which plays a crucial role in establishing the link between the unquantized data and the one-bit data regarding the auto-correlation function. By leveraging the Arcsine Law, researchers introduce the one-bit conventional beamformer (CBF) and the one-bit minimum variance distortionless response (MVDR) [7]. Subsequently, in the context of the uniform linear array (ULA) or the sparse linear array (SLA), the one-bit DoA estimation is addressed using multiple signal classification (MUSIC) based algorithms [8]–[10]. These approaches represent significant advancements, as the underlying principles of subspace techniques are utilized for improving accuracy. It is worth pointing out that they need the prior knowledge of the source number, while the classical estimators for this information (e.g., [11] and [12]) are not suitable in the one-bit case in a direct manner [13]. Moreover, the subspace-based methods require a substantial number of snapshots, especially in the case of one-bit quantization.

The conventional CS-based DoA estimation, formulated as sparse recovery, offers several advantages, including the few data samples, the low sensitivity to the signal-to-noise ratio (SNR), and the ability to handle highly correlated and coherent sources [14]. Extensive research has been devoted to CS-based one-bit DoA estimation methods, resulting in various algorithms. The complex-valued binary iterative hard thresholding (CBIHT) [15], improved CBIHT (iCBIHT) [16], atomic norm denoising (AND) [17], among others, emerge as effective techniques by capitalizing on the consistency property. The consistency property ensures that one-bit measurement preserves the same sign information as the corresponding unquantized measurement with high probability. Besides, with the aid of the Bayesian framework, generalized sparse Bayesian learning (Gr-SBL) [18] and off-grid iterative reweighted (OGIR) [4] are proposed. Furthermore, researchers address the challenges posed by non-uniform noise in one-bit DoA estimation by employing the robust sparse covariance fitting technique [19].

In this article, inspired by the likelihood-based estimation of sparse parameters (LIKES), which is a grid-based method using the maximum likelihood (ML) principle [20], we introduce a novel approach for one-bit DoA estimation of deterministic signals. The proposed method combines the strengths of ML estimation and CS, resulting in a powerful technique for the estimation of source number and DoAs. The main contributions are summarized as follows.

- 1) The ML technique is used to tackle the one-bit DoA estimation for deterministic signals.
- 2) Considering the angles of target signals have a spatial sparse property, an ML-based objective function with $\ell_{2,1}$ -norm regularization is formulated, where

the complex-valued conjugate gradient descent technique is employed to find a suitable solution with row sparsity.

Notations: We denote vectors and matrices by bold-face lower case and upper case letters, respectively. The operations $(\cdot)^H$, $(\cdot)^T$, $(\cdot)^*$, \odot and $|\cdot|$ represent conjugate transpose, transpose, conjugate, Hadamard product, and absolute value, respectively. The sets \mathbb{R} and \mathbb{C} are real-valued and complex-valued sets, respectively. Besides, \mathbf{A}_i and a_{ij} represent the i -th row vector and (i, j) entry of a matrix \mathbf{A} , respectively. Real and imaginary parts are denoted as $\Re[\cdot]$ and $\Im[\cdot]$. The $\text{diag}(\mathbf{a})$ represents a diagonal matrix whose diagonal entries are equal to the elements of \mathbf{a} . The $j = \sqrt{-1}$ stands for the imaginary unit. The $M \times M$ identity matrix is denoted by \mathbf{I}_M . The Gaussian distribution with mean \mathbf{a} and covariance matrix \mathbf{A} is denoted by $\mathcal{N}(\mathbf{a}, \mathbf{A})$. In addition, $\|\cdot\|_2$ is the ℓ_2 -norm, while $\|\mathbf{A}\|_{r,p}$ is the $\ell_{r,p}$ -norm [21], defined as

$$\|\mathbf{A}\|_{r,p} = \left[\sum_{i=1}^m \left(\sum_{j=1}^n |a_{ij}|^r \right)^{\frac{p}{r}} \right]^{\frac{1}{p}}, \quad (1)$$

where $\ell_{2,1}$ -norm is a special case of the $\ell_{r,p}$ -norm.

II. ONE-BIT SIGNAL MODEL

In this work, K far-field narrowband signals are assumed to impinge on a ULA consisting of M ($M > K$) isotropic sensors. The DoAs of these signals are represented by the vector $\boldsymbol{\theta} = [\theta_1, \theta_2, \dots, \theta_K]^T$, where $\theta_k \in [-90^\circ, 90^\circ]$ for $k = 1, 2, \dots, K$. Before quantization, the observation vector at the n -th snapshot can be expressed as

$$\mathbf{x}(n) = \tilde{\mathbf{A}}\mathbf{s}(n) + \boldsymbol{\epsilon}(n), \quad n = 1, 2, \dots, N, \quad (2)$$

where $\mathbf{s}(n) = [s_1(n), s_2(n), \dots, s_K(n)]^T \in \mathbb{C}^K$, $\boldsymbol{\epsilon}(n) = [\epsilon_1(n), \epsilon_2(n), \dots, \epsilon_M(n)]^T \in \mathbb{C}^M$, N are the deterministic but unknown signal waveforms, the additive noise, the number of snapshots, respectively. Additionally, we assume that $\boldsymbol{\epsilon}(n)$ follows a zero-mean complex circular Gaussian distribution with covariance matrix $\sigma^2 \mathbf{I}_M$, which is temporally and spatially uncorrelated with the signals. Moreover, the noise vector is independent identically distributed (i.i.d.), ensuring uncorrelated noise across time and space. Besides, $\tilde{\mathbf{A}} \in \mathbb{C}^{M \times K}$ denotes array manifold matrix which is of the form $\tilde{\mathbf{A}} = [\mathbf{a}(\theta_1), \mathbf{a}(\theta_2), \dots, \mathbf{a}(\theta_K)]$ with $\mathbf{a}(\theta_k)$ being the steering vector

$$\mathbf{a}(\theta_k) = [1, e^{j\frac{2\pi d}{\nu} \sin \theta_k}, \dots, e^{j\frac{2\pi(M-1)d}{\nu} \sin \theta_k}]^T, \theta_k \in \boldsymbol{\theta}, \quad (3)$$

where ν is the carrier wavelength and $d = \nu/2$ is the inter-element spacing.

In addition, the SNR of the k -th source signal [22] is defined as

$$\text{SNR}_k = 10 \log_{10} \left(\frac{\sum_{n=1}^N |s_k(n)|^2}{N\sigma^2} \right), \quad (4)$$

where $s_k(n)$ denotes the k -th entry of $\mathbf{s}(n)$.

When one-bit ADCs are employed, the one-bit measurement vector is given as

$$\mathbf{y}(n) = \text{sgn}(\Re[\mathbf{x}(n)]) + j\text{sgn}(\Im[\mathbf{x}(n)]), \quad (5)$$

where $\text{sgn}(\cdot)$ represents an element-wise sign function, that is

$$\text{sgn}(x) = \begin{cases} -1, & x < 0, \\ 1, & x \geq 0. \end{cases} \quad (6)$$

In this work, the aim is to estimate the DoAs $\boldsymbol{\theta}$ and the number of sources K , from the one-bit measurements $\mathbf{Y} = [\mathbf{y}(1), \mathbf{y}(2), \dots, \mathbf{y}(N)]$.

III. PROPOSED METHOD

A. One-Bit ML Formulation

Based on the assumption of the additive noise $\boldsymbol{\epsilon}(n)$ in the section II, both the real and imaginary parts of the unquantized observation $\mathbf{x}(n)$ follow Gaussian distributions, which are denoted as $\Re[\mathbf{x}(n)] \sim \mathcal{N}(\Re[\tilde{\mathbf{A}}\mathbf{s}(n)], \sigma^2/2\mathbf{I}_M)$ and $\Im[\mathbf{x}(n)] \sim \mathcal{N}(\Im[\tilde{\mathbf{A}}\mathbf{s}(n)], \sigma^2/2\mathbf{I}_M)$, respectively. Subsequently, the one-bit measurement $\mathbf{y}(n)$ follows the multivariate discrete distribution whose probability mass function (PMF) can be calculated by performing multiple integrals of the probability density function of $\Re[\mathbf{x}(n)]$ and $\Im[\mathbf{x}(n)]$ with respect to $\Re[\mathbf{x}(n)]$ and $\Im[\mathbf{x}(n)]$, respectively. The interval of integration is $[-\infty, 0]$ if any element of $\Re[\mathbf{y}(n)]$ and $\Im[\mathbf{y}(n)]$ is equal to -1 . Otherwise, it is $[0, \infty]$. As a result, the joint PMF can be given as

$$P(\mathbf{Y}; \boldsymbol{\alpha}) = \prod_{n=1}^N \prod_{m=1}^M \Phi\left(\Re[y_{mn}] \frac{\sqrt{2}\Re[\tilde{\mathbf{A}}_m \mathbf{s}(n)]}{\sigma}\right) \times \Phi\left(\Im[y_{mn}] \frac{\sqrt{2}\Im[\tilde{\mathbf{A}}_m \mathbf{s}(n)]}{\sigma}\right), \quad (7)$$

where $\boldsymbol{\alpha} = [\boldsymbol{\theta}, \sigma, \mathbf{s}(1), \dots, \mathbf{s}(N)]^T$ and $\Phi(x) = 1/\sqrt{2\pi} \int_{-\infty}^x e^{-t^2/2} dt$ are the unknown parameter vector and the cumulative distribution function of the standard normal distribution, respectively.

Then, the log-likelihood function of the one-bit observations \mathbf{Y} has the following form:

$$l(\mathbf{Y}; \boldsymbol{\alpha}) = \sum_{n=1}^N \sum_{m=1}^M \ln\left(\Phi\left(\Re[y_{mn}] \frac{\sqrt{2}\Re[\tilde{\mathbf{A}}_m \mathbf{s}(n)]}{\sigma}\right)\right) + \ln\left(\Phi\left(\Im[y_{mn}] \frac{\sqrt{2}\Im[\tilde{\mathbf{A}}_m \mathbf{s}(n)]}{\sigma}\right)\right). \quad (8)$$

It is well known that ML estimators are widely recognized for their desirable properties, such as consistency, asymptotic efficiency, and asymptotic normality [20]. Given these attractive characteristics, the ML principle is used in this work to obtain the estimates of $\boldsymbol{\theta}$. In practice, the ML estimation is achieved by minimizing the negative log-likelihood function in (8) over the parameter space, that is

$$\hat{\boldsymbol{\alpha}} = \arg \min_{\boldsymbol{\alpha}} \sum_{n=1}^N \sum_{m=1}^M f\left(\Re[y_{mn}] \Re[\tilde{\mathbf{A}}_m \mathbf{z}(n)]\right) + f\left(\Im[y_{mn}] \Im[\tilde{\mathbf{A}}_m \mathbf{z}(n)]\right), \quad (9)$$

where $\mathbf{z}(n) \triangleq \sqrt{2}\mathbf{s}(n)/\sigma$ and $f(x) \triangleq -\ln(\Phi(x))$.

However, the optimization is quite challenging to resolve due to the function $l(\mathbf{Y}; \boldsymbol{\alpha})$ is multi-modal with respect to $\boldsymbol{\theta}$. Motivated by CS theory, we cast the resultant complex optimization model into an ML-based sparse matrix recovery problem.

B. ML-Based Sparse Matrix Recovery

The potential spatial region of the incident signals is divided into a search grid of L ($K \ll L$), i.e., $\boldsymbol{\Theta} = [\phi_1, \phi_2, \dots, \phi_L]^T$, which results in an overcomplete manifold dictionary $\mathbf{A} = [\mathbf{a}(\phi_1), \mathbf{a}(\phi_2), \dots, \mathbf{a}(\phi_L)] \in \mathbb{C}^{M \times L}$. Accordingly, we construct a $L \times 1$ column vector $\mathbf{u}(n)$ which is an expanded version of $\mathbf{z}(n)$ and is defined by

$$u_l(n) = \begin{cases} z_k(n) & \text{if } \phi_l = \theta_k, l=1, 2, \dots, L, k=1, 2, \dots, K, \\ 0 & \text{otherwise,} \end{cases} \quad (10)$$

where $u_l(n)$ and $z_k(n)$ denote the l -th entry of $\mathbf{u}(n)$ and the k -th entry of $\mathbf{z}(n)$, respectively. It is seen that $\mathbf{u}(n)$ only contains K nonzero entries, whose locations correspond to the true DoAs, and therefore its sparsity is K .

With multiple data samples available, $\mathbf{u}(n)$, $n = 1, 2, \dots, N$ are jointly sparse in the sense that they share the same support. In other words, we can say that $\mathbf{U} = [\mathbf{u}(1), \dots, \mathbf{u}(N)] \in \mathbb{C}^{L \times N}$ is row sparse in the sense that it only contains K non-zero rows. Then, the optimization in (9), from the perspective of sparse signal reconstruction, can be solved by

$$\hat{\mathbf{U}} = \arg \min_{\mathbf{U}} \mathcal{L}(\mathbf{U}) + \lambda \|\mathbf{U}\|_{2,1}, \quad (11)$$

where $\mathcal{L}(\mathbf{U})$ is the likelihood term given as

$$\mathcal{L}(\mathbf{U}) = \sum_{n=1}^N \sum_{m=1}^M f\left(\Re[y_{mn}] \Re[\mathbf{A}_m \mathbf{u}(n)]\right) + f\left(\Im[y_{mn}] \Im[\mathbf{A}_m \mathbf{u}(n)]\right). \quad (12)$$

Actually, $\|\mathbf{U}\|_{2,1}$ norm is a convex function [23], approximating $\|\mathbf{U}\|_{2,0}$ norm to enforce a row sparse solution. In addition, $\lambda > 0$ is a regularization parameter to trade off the fidelity of the likelihood term and the row sparsity of matrix.

It is observed that the objective function in (11) is convex, indicating that traditional tools, such as CVX [24], can be utilized to solve it. However, the CVX employs the interior point technique to handle such kind of problems, and thus its computational complexity is relatively high.

To address this issue, as an unconstrained optimization, the problem in (11) can be solved via the steepest descent method [25], that is

$$\mathbf{U}^{r+1} = \mathbf{U}^r + \eta \Delta \mathbf{U}, \quad (13)$$

where r , η , and $\Delta \mathbf{U}$ denote the r -th iteration, the step size, and the steepest descent direction, respectively. The convergence of our method using the conjugate gradient

descent framework is guaranteed [25]. Furthermore, ΔU is the negative conjugate gradient of $\mathcal{L}(U) + \lambda \|U\|_{2,1}$, which is derived as follows.

Actually, [26] has provided the derivatives of $\|U\|_{2,1}$ with respect to U^* , i.e.,

$$\frac{\partial \|U\|_{2,1}}{\partial U^*} = \frac{1}{2} DU, \quad (14)$$

where $D \in \mathbb{R}^{L \times L}$ is a diagonal matrix related to $\|U_l\|_2$, $l = 1, 2, \dots, L$, i.e.,

$$D = \text{diag} \left(\frac{1}{\|U_1\|_2}, \frac{1}{\|U_2\|_2}, \dots, \frac{1}{\|U_L\|_2} \right). \quad (15)$$

When $U_l = \mathbf{0}$, $d_{ll} = 0$ is a conjugate subgradient of $\|U\|_{2,1}$ with respect to U_l [23].

Regarding the derivatives of $\mathcal{L}(U)$ with respect to U^* , we firstly take the partial derivative of $\mathcal{L}(U)$ with respect to u_{pq}^* , that is

$$\begin{aligned} \frac{\partial \mathcal{L}(U)}{\partial u_{pq}^*} &= \sum_{n=1}^N \sum_{m=1}^M f'(\Re[y_{mn}] \Re[\mathbf{A}_m \mathbf{u}(n)]) \Re[y_{mn}] \frac{\partial \Re[\mathbf{A}_m \mathbf{u}(n)]}{\partial u_{pq}^*} \\ &\quad + f'(\Im[y_{mn}] \Im[\mathbf{A}_m \mathbf{u}(n)]) \Im[y_{mn}] \frac{\partial \Im[\mathbf{A}_m \mathbf{u}(n)]}{\partial u_{pq}^*}, \end{aligned} \quad (16)$$

where the derivative of $f(x)$ is denoted as

$$f'(x) = -\frac{1}{\sqrt{2\pi}\Phi(x)} e^{-\frac{x^2}{2}}. \quad (17)$$

Then, considering the identities $\Re[\mathbf{A}_m \mathbf{u}(n)] = \Re[\mathbf{A}_m] \Re[\mathbf{u}(n)] - \Im[\mathbf{A}_m] \Im[\mathbf{u}(n)]$ and $\Im[\mathbf{A}_m \mathbf{u}(n)] = \Re[\mathbf{A}_m] \Im[\mathbf{u}(n)] + \Im[\mathbf{A}_m] \Re[\mathbf{u}(n)]$, and using the Wirtinger's calculus [27], we have

$$\begin{aligned} \frac{\partial \Re[\mathbf{A}_m \mathbf{u}(n)]}{\partial u_{pq}^*} &= \frac{1}{2} \frac{\partial \Re[\mathbf{A}_m \mathbf{u}(n)]}{\partial \Re[u_{pq}]} + \frac{j}{2} \frac{\partial \Re[\mathbf{A}_m \mathbf{u}(n)]}{\partial \Im[u_{pq}]} \\ &= \frac{1}{2} \frac{\partial \Re[\mathbf{A}_m] \Re[\mathbf{u}(n)]}{\partial \Re[u_{pq}]} - \frac{j}{2} \frac{\partial \Im[\mathbf{A}_m] \Im[\mathbf{u}(n)]}{\partial \Im[u_{pq}]} \\ &= \frac{1}{2} \frac{\partial \sum_{j=1}^L \Re[a_{mj}] \Re[u_{jn}]}{\partial \Re[u_{pq}]} - \frac{j}{2} \frac{\partial \sum_{j=1}^L \Im[a_{mj}] \Im[u_{jn}]}{\partial \Im[u_{pq}]} \\ &= \frac{1}{2} \Re[a_{mp}] - \frac{j}{2} \Im[a_{mp}] = \frac{1}{2} a_{mp}^*. \end{aligned} \quad (18)$$

Note that the last equality holds only when $n = q$.

Similarly, we have

$$\frac{\partial \Im[\mathbf{A}_m \mathbf{u}(n)]}{\partial u_{pq}^*} = \frac{j}{2} a_{mp}^*. \quad (19)$$

Next, substituting (18) and (19) into (16), we obtain

$$\begin{aligned} \frac{\partial \mathcal{L}(U)}{\partial u_{pq}^*} &= \sum_{m=1}^M \frac{a_{mp}^*}{2} f'(\Re[y_{mn}] \Re[\mathbf{A}_m \mathbf{u}(n)]) \Re[y_{mn}] \\ &\quad + j \frac{a_{mp}^*}{2} f'(\Im[y_{mn}] \Im[\mathbf{A}_m \mathbf{u}(n)]) \Im[y_{mn}]. \end{aligned} \quad (20)$$

Finally, the conjugate gradient matrices $\partial \mathcal{L}(U) / \partial U^*$ can be derived as

$$\begin{aligned} \frac{\partial \mathcal{L}(U)}{\partial U^*} &= \frac{1}{2} \mathbf{A}^H f'(\Re[\mathbf{Y}] \odot \Re[\mathbf{A}U]) \odot \Re[\mathbf{Y}] \\ &\quad + \frac{j}{2} \mathbf{A}^H f'(\Im[\mathbf{Y}] \odot \Im[\mathbf{A}U]) \odot \Im[\mathbf{Y}]. \end{aligned} \quad (21)$$

Combining (14) and (21), we can obtain the steepest descent direction

$$\begin{aligned} \Delta U &= -\frac{1}{2} \mathbf{A}^H f'(\Re[\mathbf{Y}] \odot \Re[\mathbf{A}U]) \odot \Re[\mathbf{Y}] \\ &\quad - \frac{j}{2} \mathbf{A}^H f'(\Im[\mathbf{Y}] \odot \Im[\mathbf{A}U]) \odot \Im[\mathbf{Y}] - \frac{\lambda}{2} DU. \end{aligned} \quad (22)$$

After R iterations, the solution \hat{U} is obtained, and then the normalized spatial power spectral (NSPS) $p(l)$ is calculated using the following expression

$$p(l) = \frac{\|\hat{U}_l\|_2^2}{\max_{l=1,2,\dots,L} \|\hat{U}_l\|_2^2}, l = 1, 2, \dots, L. \quad (23)$$

Subsequently, the DoAs of the source signals can be determined by identifying the peaks corresponding to $p(l)$. The location of peaks in $p(l)$ indicates the directions from which the signals originate. Therefore, the number of peaks corresponds to the estimated number of source signals. Because the noise may generate peaks corresponding to many false alarms with small magnitude, we set a threshold, half of the maximum peak of NSPS, to filter these peaks. Certainly, there are alternative choices for thresholding, including adaptive methods, which is beyond the scope of this work. The procedure is summarized in Algorithm 1.

Algorithm 1: One-bit ML based sparse matrix recovery

Input: One-bit observation \mathbf{Y} , number of antennas M , number of grids L , number of iterations R , and step size η .

Step 1. $r = 0$, the elements of Θ are L values uniformly sampled from -90° to 90° , and $U^0 \in \mathbb{C}^{L \times N} \leftarrow$ a random matrix.

for $r = 1, 2, \dots, R$ **do**

Step 2. Determine ΔU by (22).

Step 3. Update U^{r+1} by (13).

end for

Step 4. Calculate NSPS by (23) and then obtain $\hat{\theta}$ and \hat{K} by finding and counting the peaks of NSPS.

Output: $\hat{\theta}$, \hat{K} .

The computational complexity (CC) of the proposed method mainly comes from the update of (13). In each iteration, the CC of (14) is $\mathcal{O}(LN)$, which is because that the CC of the calculation of diagonal matrix D is $\mathcal{O}(LN)$, and the CC of DU is also $\mathcal{O}(LN)$. Additionally, the CC of (21) is $\mathcal{O}(MLN)$, mainly coming from the calculation of $\mathbf{A}U$. As a result, the total CC of our method is $\mathcal{O}(RMLN)$, where R represents the number of iterations.

IV. SIMULATION RESULTS

In this simulation, a ULA comprising $M = 15$ antennas with a half-wavelength inter-element spacing is considered. The ULA receives three signal waveforms from distinct directions $\theta = [-33^\circ, 2^\circ, 23^\circ]^T$. These signal

waveforms are represented as complex-valued exponential signals, i.e., $\mathbf{s}(n) = [e^{j/30n}, e^{j/6n}, e^{j/15n}]^T$. Besides, the potential spatial region of the incident signals is set from -90° to 90° and a uniform discretization with a grid size of 0.1° over the spatial region is operated to obtain set Θ , i.e., $L = 1801$. In the steepest descent method, the size step η and the number of iterations R are set as 0.1 and 500. To evaluate the estimation performance, the root mean square error (RMSE) of θ is adopted as the metric, defined as

$$\text{RMSE} = \sqrt{\frac{1}{100K} \sum_{j=1}^{100} \sum_{k=1}^K (\theta_k - \hat{\theta}_{j,k})^2}, \quad (24)$$

where $\hat{\theta}_{j,k}$ is the estimate of the k -th DoA in the j -th trial.

For comparison purposes, four existing algorithms are evaluated, namely, One-bit MUSIC [9], AND [17], Gr-SBL [18], and OGIR [4]. Additionally, the Cramer-Rao Bound (CRB) [28, Eq.(18)], acted as the benchmark, is included. In the following examples 1–4, the source number is assumed to be known.

As mentioned earlier, the regularization parameter λ governs the trade-off between the fidelity of the likelihood term and the row sparsity of the matrix. A larger value of λ results in a more row-sparse \mathbf{U} . In contrast, a smaller λ value leads to a less row-sparse \mathbf{U} but results in a better fitting of the likelihood term $\mathcal{L}(\mathbf{U})$. However, to the best of our knowledge, determining a general rule for selecting the appropriate regularization parameter in DoA estimation remains an open issue [14]. In our work, we provide a rule of thumb to guide the selection of λ based on simulation results [25]. These simulations provide valuable insights into the impact of different λ values on the performance of the one-bit DoA estimation under various scenarios.

Example 1: First, RMSE curves versus the regularization parameter λ in the cases of different SNRs, are plotted in Fig. 1, where the number of snapshots is set as 20. It is obvious that the optimal regularization parameter is sensitive to the SNRs especially at lower SNRs. To ensure optimal performance under different SNR conditions, we carefully select specific λ values for every SNR. Specifically, we choose $\lambda = 19, 20, 24, 24, 24, 24$ corresponding to the SNRs = $-10, -6, -2, 2, 6, 10$, respectively, for the subsequent evaluation tests.

Example 2: Then, we examine the RMSE performance of the proposed method and some existing methods in terms of SNR. As shown in Fig. 2, it is evident that the RMSEs of all tested methods decrease as the SNR increases and the proposed method outperforms the other algorithms in the tested SNR range. Besides, the other examined approaches exhibit relatively similar and worse estimation accuracy, particularly when SNR is lower than -2 dB. The superiority of the proposed method becomes more apparent as the SNR increases. When the SNR is larger than 2 dB, the proposed method attains the CRB,

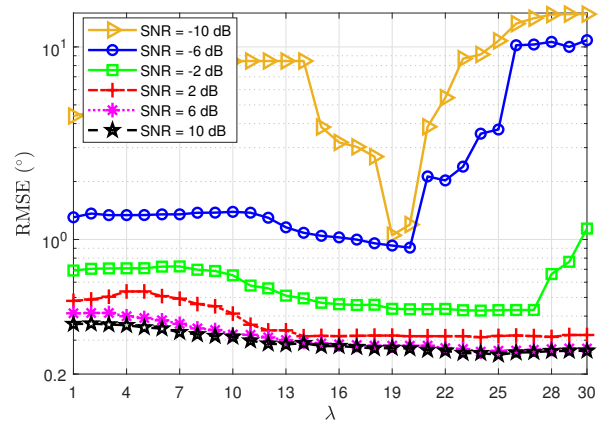


Fig. 1. RMSE versus regularization parameter λ for various SNRs.

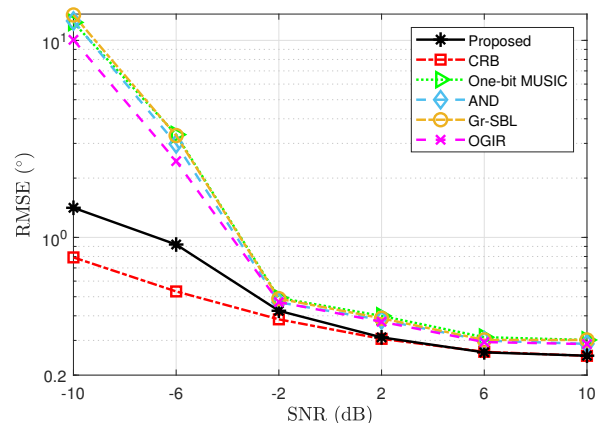


Fig. 2. RMSE versus SNR.

which indicates that the proposed approach reaches the theoretical lower bound of estimation accuracy.

Example 3: In this part, Fig. 3 reveals the RMSE curves versus the regularization parameter λ under different numbers of snapshots, for SNR = 0 dB. It is seen that when the number of snapshots is greater than 80, the selection of λ has a slight effect on the RMSE. To obtain the optimal λ corresponding to each tested number of snapshots, the minimal value is identified on every curve. It is worth noting that there is a consistent trend that as the number of snapshots increases by 20, the approximate optimal value of λ increases by 1. Consequently, λ is set as 19 when the number of snapshots is 20, and then each time that the number of snapshots grows by 20, λ increases by 1 in the following evaluation.

Example 4: Finally, the RMSEs of all tested methods mentioned above versus the number of snapshots are investigated. The results are plotted in Fig. 4. It is seen that the performance of the proposed method stands out as superior to the other algorithms and the Gr-SBL is the worst one. Moreover, the performance of the proposed method closely approaches the CRB. This finding underscores the effectiveness of the proposed approach.

Example 5: To assess the performance of the proposed method in terms of the source number estimation, we examine the probability of success (PoS) versus SNR. The

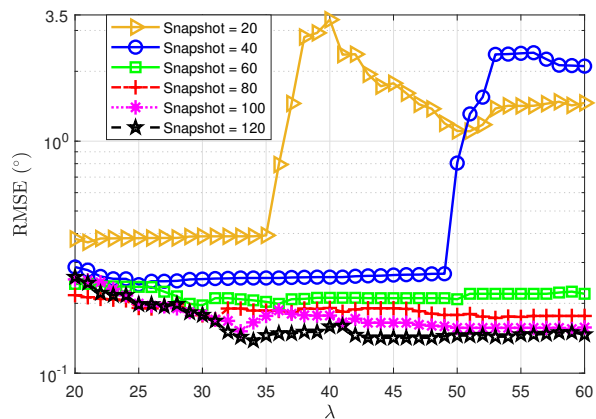


Fig. 3. RMSE versus regularization parameter λ for various numbers of snapshots.

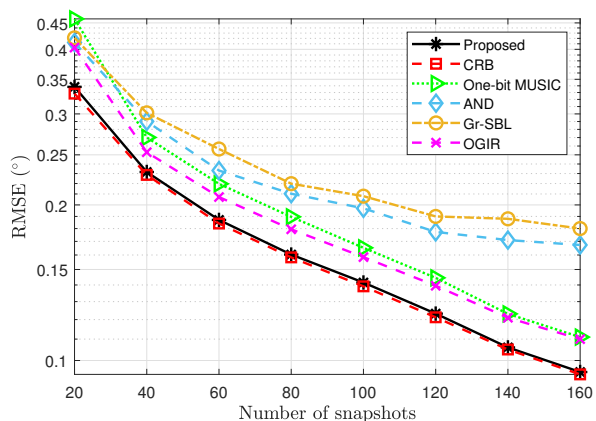


Fig. 4. RMSE versus numbers of snapshots.

PoS is the ratio of successful tests to total tests. The test is considered successful if the estimates of source number \hat{K} equal the ground truth. Since either One-bit MUSIC or AND requires the prior knowledge of the source number, they are not tested in this example for comparison.

The tested results are plotted in Fig. 5. As expected, the PoS of all methods increases with increasing SNR, and the proposed method maintains the best performance among all tested compared methods. Notably, our algorithm reaches almost 100% in the case of SNR > 2 dB, demonstrating its effectiveness in estimating the number of sources.

V. CONCLUSION

In this paper, the one-bit DoA estimation for deterministic signal was studied. A novel method that integrates the ML principle and sparse recovery technique was proposed to estimate source number and DoAs simultaneously. The numerical experiments demonstrated its superiority over existing state-of-the-art one-bit approaches in terms of estimation accuracy. Our method consistently had the highest accuracy in a range of SNR and snapshot scenarios. Moreover, the proposed method attained the CRB in high SNR regimes and large snapshot scenarios, affirming

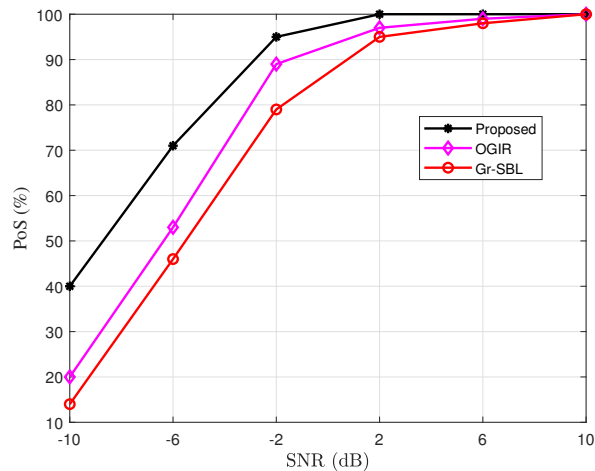


Fig. 5. PoS versus SNR.

its effectiveness in approaching the theoretical lower bound of estimation accuracy. One challenge in this work involved the selection of the regularization parameter, which requires careful consideration through simulation experiments. To overcome this, we plan to develop a hyperparameter-free approach in future research.

Mingyang Chen, Qiang Li, Xiao Peng Li
Shenzhen University, Shenzhen 518060, China

Lei Huang, Senior Member, IEEE
State Key Laboratory of Radio Frequency
Heterogeneous Integration (Shenzhen
University), Shenzhen 518060, China

Mohamed Rihan, Senior Member, IEEE
University of Bremen, Germany

REFERENCES

- [1] X. Chen, L. Huang, H. Zhou, Q. Li, K.-B. Yu, and W. Yu One-bit digital beamforming *IEEE Trans. Aerosp. Electron. Syst.*, vol. 59, no. 1, pp. 555–567, Feb. 2023.
- [2] X. P. Li, Z. Liu, Z.-L. Shi, and H. C. So MUSIC with capped frobenius norm: Efficient robust direction-of-arrival estimator *IEEE Trans. Aerosp. Electron. Syst.*, Early Access 2023, doi:10.1109/TAES.2023.3300264.
- [3] Z. Liu, X. P. Li, and H. C. So ℓ_0 -norm minimization-based robust matrix completion approach for mimo radar target localization *IEEE Trans. Aerosp. Electron. Syst.*, vol. 59, no. 5, pp. 6759–6770, Oct. 2023.
- [4] L. Feng, L. Huang, Q. Li, Z.-Q. He, and M. Chen An off-grid iterative reweighted approach to one-bit direction of arrival estimation *IEEE Trans. Veh. Technol.*, vol. 72, no. 6, pp. 8134–8139, Jan. 2023.
- [5] J. H. Van Vleck and D. Middleton The spectrum of clipped noise *Proc. IEEE*, vol. 54, no. 1, pp. 2–19, Jan. 1966.
- [6] G. Jacovitti and A. Neri Estimation of the autocorrelation function of complex gaussian stationary processes by amplitude clipped signals *IEEE Trans. Inf. Theory*, vol. 40, no. 1, pp. 239–245, Jan. 1994.
- [7] O. Bar-Shalom and A. J. Weiss

- DOA estimation using one-bit quantized measurements
IEEE Trans. Aerosp. Electron. Syst., vol. 38, no. 3, pp. 868–884, Jul. 2002.
- [8] C.-L. Liu and P. P. Vaidyanathan
One-bit sparse array DOA estimation
In *Proc. IEEE Int. Conf. Acoust., Speech, Signal Process.*, New Orleans, LA, USA, Mar. 2017, pp. 3126–3130.
- [9] X. Huang and B. Liao
One-bit MUSIC
IEEE Signal Process. Lett., vol. 26, no. 7, pp. 961–965, Jul. 2019.
- [10] S. Sedighi, B. S. M. R. M. Soltanalian, and B. Ottersten
On the performance of one-bit DoA estimation via sparse linear arrays
IEEE Trans. Signal Process., vol. 69, pp. 6165–6182, Oct. 2021.
- [11] L. Huang, S. Wu, and X. Li
Reduced-rank MDL method for source enumeration in high-resolution array processing
IEEE Trans. Signal Process., vol. 55, no. 12, pp. 5658–5667, Dec. 2007.
- [12] L. Huang and H. C. So
Source enumeration via MDL criterion based on linear shrinkage estimation of noise subspace covariance matrix
IEEE Trans. Signal Process., vol. 61, no. 19, pp. 4806–4821, Oct. 2013.
- [13] M. Chen, Y.-H. Xiao, Q. Li, L. Feng, M. Rihan, and N. Guo
One-bit source number detection via neural network
In *Int. Conf. Inf. Commun. Signal Process.*, Shenzhen, China, Nov. 2022, pp. 91–95.
- [14] J. Fang, F. Wang, Y. Shen, H. Li, and R. S. Blum
Super-resolution compressed sensing for line spectral estimation: An iterative reweighted approach
IEEE Trans. Signal Process., vol. 64, no. 18, pp. 4649–4662, Sep. 2016.
- [15] C. Stöckle, J. Munir, A. Mezghani, and J. A. Nossek
1-bit direction of arrival estimation based on compressed sensing
In *16th IEEE Workshop Signal Process. Adv. Wireless Commun.*, Stockholm, Sweden, Jul. 2015, pp. 246–250.
- [16] P. Wang, H. Yang, and Z. Ye
1-bit direction of arrival estimation via improved complex-valued binary iterative hard thresholding
Digit. Signal Process., vol. 120, p. 103265, Jan. 2022.
- [17] Z. Wei, W. Wang, F. Dong, and Q. Liu
Gridless one-bit direction-of-arrival estimation via atomic norm denoising
IEEE Commun. Lett., vol. 24, no. 10, pp. 2177–2181, Oct. 2020.
- [18] X. Meng and J. Zhu
A generalized sparse bayesian learning algorithm for 1-bit DOA estimation
IEEE Commun. Lett., vol. 22, no. 7, pp. 1414–1417, Jul. 2018.
- [19] M. Chen, Q. Li, L. Huang, L. Feng, M. Rihan, and D. Xia
One-bit DOA estimation using robust sparse covariance fitting in non-uniform noise
In *Proc. 12th Sensor Array and Multichannel Signal Process. Workshop*, Trondheim, Norway, Jun. 2022, pp. 11–15.
- [20] P. Stoica and P. Babu
SPICE and LIKES: Two hyperparameter-free methods for sparse-parameter estimation
Signal Process., vol. 92, no. 7, pp. 1580–1590, Jul. 2012.
- [21] C. Ding, D. Zhou, X. He, and H. Zha.
R1-PCA : rotational invariant ℓ_1 -norm principal component analysis for robust subspace factorization
In *Pro. 23th Conf. Machine Learning*, Pittsburgh, Jun 2006, pp. 281–288.
- [22] N. Zhang, J. Zhu, and Z. Xu
Gridless multisnapshot variational line spectral estimation from coarsely quantized samples
IEEE Trans. Aerosp. Electron. Syst., vol. 59, no. 3, pp. 2979–2993, Nov. 2022.
- [23] F. Nie, H. Huang, X. Cai, and C. H. Ding
Efficient and robust feature selection via joint $\ell_{2,1}$ -norms minimization
In *Proc. 23th Conf. Advance Neural Inf. Process. Syst.*, Vancouver, British Columbia, Canada, Dec. 2010, pp. 1813–1821.
- [24] M. Grant and S. Boyd
CVX: Matlab software for disciplined convex programming, version 2.1
[Online], Mar. 2014, Available: <http://cvxr.com/cvx>.
- [25] S. Boyd and L. Vandenberghe
Convex Optimization. U.K., Cambridge: Cambridge Univ. Press, 2004.
- [26] Q. Li, L. Huang, W. Liu, X. Chen, and L. Feng
Cold-start satellite signal acquisition aided by an antenna array in the presence of outliers
IEEE Trans. Veh. Technol., vol. 72, no. 5, pp. 5847–5861, May 2023.
- [27] R. Remmert
Theory of Complex Functions. USA, New York: Springer-Verlag, 1991.
- [28] M. Chen, Q. Li, L. Huang, L. Feng, and M. Rihan
One-bit Cramér–Rao Bound of direction of arrival estimation for deterministic signals
IEEE Trans. Circuits Syst. II Exp. Briefs, Early Access 2023, doi:[10.1109/TCSII.2023.3309788](https://doi.org/10.1109/TCSII.2023.3309788).